Int. J. Nonlinear Anal. Appl.
Volume 12, Special Issue, Winter and Spring 2021, 1059-1074
ISSN: 2008-6822 (electronic)
http://dx.doi.org/10.22075/IJNAA.2021.5569

Voltage boosting capability of three phase current source inverter for standalone system

Chong Sin Yee[a], Syahrul Ashikin Azmi[a,*], Leong Jenn Hwai[a], Grain Adam[b], Siti Rafidah Abdul Rahim[a]

[a]*Faculty of Electrical Engineering Technology, Universiti Malaysia Perlis, Perlis, Malaysia.*
[b]*EOM Company, Tabuk, Saudi Arabia.*

(Communicated by Madjid Eshaghi Gordji)

Abstract

This paper presents a three-phase current source inverter (CSI) topology with voltage boosting capability for standalone system. Current source inverter (CSI) and voltage source inverter (VSI) are two competitive options to be used as an interfacing unit between variable dc input resource and ac output fed into on-grid, off-grid and industrial used. Among the two topologies, VSI is widely used due to its variable controllable output voltage and ability to operate steadily with open loop V/Hz control. Yet, it suffers circuit complexity due to the need of extra converter stage to meet the required output. On the other hand, CSI has an advantage of voltage boosting capability and better quality of output waveshape, thus no extra converter stage is needed. Most of research works were focusing on studying the suitability and practicality of CSI, along with the advancement using silicon carbide-based power switches and improved modulation techniques to minimize the harmonics suffer by CSI. There is lack of research in investigating the boosting capability particularly on how high CSI able to boost the fundamental output and its impact to overall performance in both open and closed-loop standalone system. Thus, this work is intended to highlight in detail the boosting capability of CSI and compare with VSI based on the several circuity and operational features. To support the work, three modulators are implemented namely sinusoidal pulse width modulation (SPWM), third harmonic injection PWM (THIPWM) and space vector modulation (SVM). A dedicated synchronous frame proportional-integral (PI) control in used in closed-loop condition. Result shows that CSI topology able to boost the fundamental output voltage by 52% to 58% by using smaller modulation index as compared to VSI. Interestingly, CSI able to achieve comparable quality and harmonic minimization of output voltage and current as in VSI but with smaller PI control gain. All works are analyzed and verified using MATLAB/Simulink platform.

Keywords: Voltage source inverter (VSI), Current source inverter (CSI), SPWM, THIPWM, SVM, Voltage-controlled inverter, Comparative analysis

*Corresponding author
Email addresses: siny0712@gmail.com (Chong Sin Yee), ashikin@unimap.edu.my (Syahrul Ashikin Azmi), jhleong@unimap.edu.my (Leong Jenn Hwai), rafidah@unimap.edu.my (Grain Adam), grain.adam2010@gmail.com (Siti Rafidah Abdul Rahim)

Received: June 2021 *Accepted:* September 2021

1. Introduction

An inverter is the heart of an electrical power generation system. It plays an important role to converts the direct current (DC) output into alternating current (AC) output at the desired output voltage and frequency. Inverter can be classified as voltage source inverter (VSI) and current source inverter (CSI) based on their input sources. These two types of inverters provide significant advantages in respective industrial usage. VSI is widely used due to its variable controllable output voltage and ability to operate steadily with open loop V/Hz control [1]. Moreover, nowadays VSI design is fully integrated into a chip which have higher efficiencies, higher reliability, faster dynamic response, low cost and minimizing the install time [18]. However, the output of three-phase VSI has high total harmonic distortion (THD) which may cause overheating and damage on the load or system [2].

Current source inverter (CSI) on the other hand able to provide high quality voltage or current waveform output for industrial applications. Yet it suffers drawbacks such as high conduction losses, high power losses and high in cost [6, 11]. These high-power losses issues affect the efficiency of three-phase CSI and this make it uncommercial option as VSI. Interestingly, the DC-link component of CSI which is dc-link inductor has the inherent characteristics of voltage boosting. This characteristic able to boost the output voltage of the inverter, whereby reduces the usage of a DC-DC boost converter which is compulsory for VSI. This decreases the circuit complexity of the system [9].

VSI is known to has buck operation function while CSI has boost operation function. This is supported by the fact that VSI output voltage peak value is always lower than the input dc voltage [19]. On the other hand, CSI has an output voltage peak value is higher than the input dc voltage, thus it may become an alternative topology to replace the VSI in some applications. CSI can achieve better performance in term of motor efficiency, insulation stress and common-mode voltage for low power induction motor [13]. For medium-voltage industrial applications, CSI is less efficiency than VSI due to the higher losses at the snubbers and dc-link choke inductors [19]. For high power industrial applications (rated power $\geq$ 20MW), load-commutated CSI is comparable with VSI for non-regenerative low dynamic requirement applications, however, VSI still achieves higher efficiency than CSI for the regenerative applications [19, 13, 10].

In aspect of losses analysis, it is discovered that CSI has lower switching losses compared to VSI, thus lead to an advantage of lower total power losses at high switching frequency according to [7]. The introduction of silicon carbide (SiC) based power switches into CSI also an enhancement on this advantage. SiC power switches able to work at high frequency and high temperature, and it have lower activation and conduction losses compared to conventional IGBT power switches [4]. These characteristic of SiC power switches promote that CSI to have lower total power losses and higher efficiency [8]. CSI also become an optimal choice for high-speed applications. In [12], it shown that CSI-STATCOM (static compensator) available to provide higher efficiency with smaller sizing and cost compared to VSI-STATCOM in high-speed railway substations. Moreover, a recent study by [5] also concluded that CSI suitable for variable-speed drive with a wide operating range, especially at high speeds, while VSI suitable for low-speed applications for example macro scale electrostatic machines, it can provide high efficiency over a wide operating range with proper filter design.

Although CSI topology is extensively studied in the literature, there are lack of research in highlighting the fundamental understanding on the operational features of CSI over VSI topology. As mentioned in most papers on the boosting capability of CSI, but how much boosting do CSI able to provides and the impact of this feature to the other parameters in the system are vague. Thus, this paper is aimed to highlight the inherent feature comprehensively, relate it with the modulation index, fundamental output voltage and harmonic minimization by using three modulation techniques

as the modulators or control unit. In addition, a dedicated improved control design consists of a voltage-control loop is proposed to strengthen the analysis of CSI in open and closed-loop standalone system This work is beneficial as a guidance in selecting the suitable topology and related operational parameters as well as able to fully utilize the boosting capability and smaller control gain of CSI in serving the intended application. All circuits and control units are constructed and verified using MATLAB/Simulink platform.

2. Theoretical background and modulation techniques of VSI and CSI

2.1. Power circuit

Figure 1 and 2 present the basic topologies of VSI and CSI. Looking at power circuit of the inverters at dc-input side, VSI input voltage is maintained as constant and input current is variable while in CSI, the input current is maintained as constant and input voltage is variable. Since the input current of three-phase CSI is maintained constant, it brings advantage on limiting the peak current of power switches, thus reduce the misfiring of power switches which may cause short circuit [17]. VSI required a dc-link capacitor to regulate the input dc voltage stability while CSI required a dc-link inductor to regulate the input dc current stability. These dc-passive components affected the turning sequence of power switches in three-phase VSI and CSI. A dead time is required in the switching control for three-phase VSI to prevent a short circuit at the dc side while an overlap time is required switching control for three-phase CSI to prevent an open circuit occurs at the dc side [17, 20]. Thus, it is easier to fulfil the switching requirement of three-phase CSI in practical implementation.

For the output side, VSI provides a controlled ac voltage output which is independently on the loads. However, its ac current output is dependent on the loads. In three-phase CSI, it provides controlled ac current output which is independently on loads, but its ac voltage output is depends upon the loads. VSI has buck operation function while three-phase CSI has boost operation function [20]. A three-phase VSI output voltage peak value is always lower than the input dc voltage. Therefore, it normally required a dc-dc boost converter or step-up transformer to boost up its input dc voltage in order to generate the required output voltage [20]. For three-phase CSI, its output voltage peak value is higher than the input dc voltage. This present that three-phase CSI inherent voltage boosting capability which becomes the distinct feature for CSI as compared to VSI. A summary of comparison between both VSI and CSI is presented in Table 1.

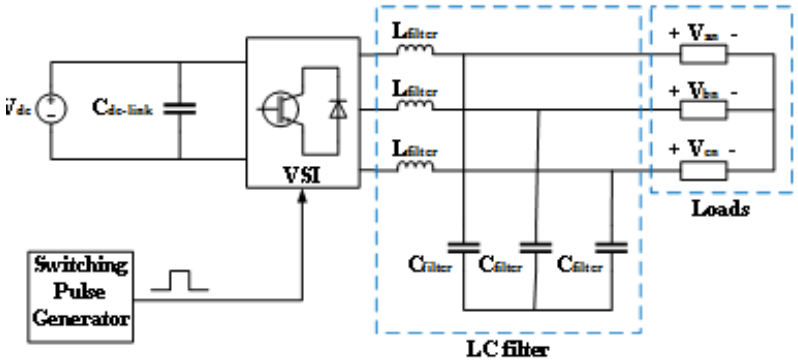

Figure 1: Voltage source inverter topology with LC-power filters

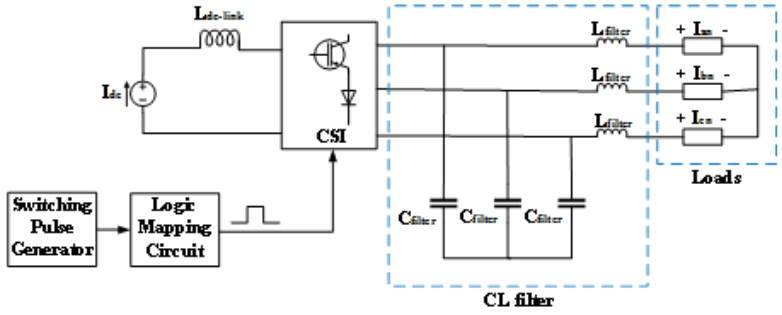

Figure 2: Current source inverter topology with CL-filters

2.2. Modulation techniques

A. Sinusoidal Pulse Width Modulation (SPWM) technique

Three sinusoidal reference waves ($v_{ra}, v_{rb}, and v_{rc}$) each shifted by 120° are compared with a triangular carrier wave (v_{cr}) to generate gating signals corresponding to each phase. Each sinusoidal reference waves are corresponding to a phase and its frequency determined the fundamental frequency of output while the triangular carrier wave's frequency determine the switching frequency. For SPWM three-phase VSI, the peak amplitude of fundamental phase voltage and line-to-line voltage are written as equations (1) and (2) [14].

$$V_{phase,peak} = m_a(\frac{V_{dc}}{2}),\ 0 \leq m_a \leq 1 \tag{1}$$

$$V_{L-L,peak} = m_a\sqrt{3}(\frac{V_{dc}}{2}),\ 0 \leq m_a \leq 1 \tag{2}$$

B. Third harmonic injection pulse width modulation (THIPWM) technique

A third harmonic injection modulating signal is added with the fundamental modulating signal, thus result as a THIPWM reference signal, vref,THIPWM which is not sinusoidal and it can expressed as equation (3) [3].

$$F(x) = v_{ref.THIPWM} = \frac{2}{\sqrt{3}}sin(x) + \frac{1}{3\sqrt{3}}sin(3x) \tag{3}$$

The $v_{ref,THIPWM}$ consists of fundamental component and third harmonic component, its peak-to-peak amplitude does not exceed the dc supply voltage however its fundamental component is higher than the available dc supply voltage. For THIPWM three-phase VSI, the peak amplitude of fundamental phase voltage and line-to-line voltage can be written as equations (4) and (5).

$$V_{phase,peak} = m_a(\frac{V_{dc}}{\sqrt{3}}),\ 0 \leq m_a \leq 1 \tag{4}$$

$$V_{L-L,peak} = m_a V_{dc},\ 0 \leq m_a \leq 1 \tag{5}$$

C. Space vector modulation (SVM) technique

Space vector modulation is based on eight possible switch state combinations for a three-phase VSI. A switch constraint for the VSI is that each leg contains two series switching devices operating

Table 1: Comparative analysis of three-phase VSI and CSI in term of power circuit

	VSI	CSI
Dc input	• Input voltage is constant. • Input current is variable.	• Input current is constant. • Input voltage is variable.
Ac output	• Controllable ac voltage output. Ac current output is dependent on loads.	• Controllable ac current output. • Ac voltage output is dependent on loads.
Dc-link passive component	• Dc-link capacitor to regulate the input dc voltage stability.	• Dc-link inductor to regulate the input dc current stability.
Switching requirement	• A dead time is required in the switching control to prevent a short circuit at the dc side.	• An overlap time is required in switching control to prevent an open circuit occurs at the dc side.
Buck or boost characteristic	• Buck operation function. • Dc-dc boost converter is normally required.	• Boost operation function. • Inherit voltage boosting capability.
Advantages	• Ease to control due to its output voltage is independently on the loads. • Have low conduction losses. • Ability to operate steadily with open loop V/Hz control.	• Misfiring of power switches issues can be reduced due to limited input peak current. • The power switches switching requirement is easier to be implemented in practical. • Have lower switching losses and higher calculated inductor power density. • Implicit over-current protection ability.
Drawbacks	• The power switches switching requirement is hard to control and implemented in practical. • Additional of dc-dc boost converter or step-up transformer increase the circuit complexity and cost.	• Have high conduction losses.

in a complementary manner. If the upper switch is turned on, the corresponding lower switch is off, and vice versa [16].

The space vector diagram for a two-level inverter is shown in Figure 3. There are six stationery active vectors, namely $\overline{V_1}$ to $\overline{V_6}$, zero vector $\overline{V_0}$ and the reference vector, $\overline{V_{ref}}$ that rotate in space at an angular velocity of the fundamental frequency of the inverter voltage [15].

The dwell times for the stationery vectors represents the duty-cycle time (on-state or off-state time) of the chosen switches during a sampling period T_s for all six sectors that can be calculated as in (6):

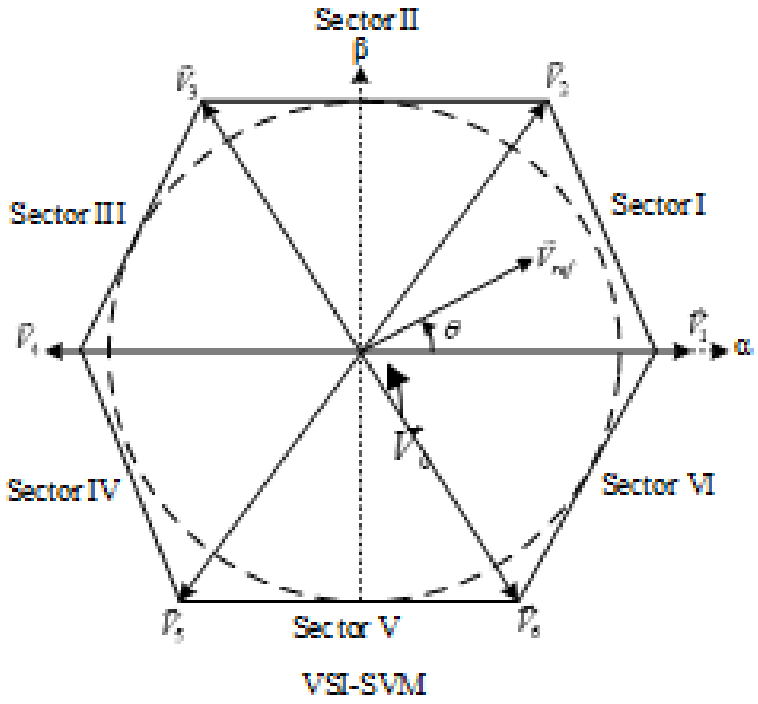

Figure 3: Space vector diagram for a two-level inverter.

$$
\begin{aligned}
T_1 &= m_a T_s sin\left|\left(\frac{n\pi}{3} - \theta\right)\right. \\
T_2 &= m_a T_s sin\left|\left(\theta - \frac{(n-1)\pi}{3}\right)\right. \\
T_0 &= T_s - T_1 - T_2 \qquad (6)
\end{aligned}
$$

where $m_a = \frac{2}{\sqrt{3}} \frac{V_{ref}}{V_{dc}}$ is amplitude modulation index and n is the sector number.

For three-phase CSI, the SPWM, THIPWM and SVM techniques are extended from three-phase VSI by adding logic mapping circuit. The implementation of these modulation techniques in controlling the fundamental output in open-loop condition is explained in subsequent section.

3. Methodology of dedicated modulator and voltage-controlled system for the inverter system

3.1. Design of control modulators for open-loop condition

Figures 4, 5 and 6 present the implementation of three modulators as the control unit for the inverter system. Figure 4 illustrates the design of SPWM modulator using three reference signals based on equation (1) and compared with a single high-frequency carrier signal. The 'high' and 'low' outputs generated by these signal intersections are placed and arranged to a combination of upper and bottom switches. This is to ensure minimal switch transition occurred in each 1/6 or 60° cycle over one switching period. Taking similar principle as SPWM, Figure 5 add third harmonic component in the reference signal as stated in equation (3) and (4) to increase the fundamental output by 15.5%.

The reference signals are compared with a high frequency carrier signal to generate the train of pulses. THIPWM technique enables better utilization of dc input and harmonic compensation as compared to SPWM. Figure 6 shown the implementation of SVM as the modulator based on Figure 3 and equation (6). It also offers flexibility in terms of pulse placement in any of the dedicated sectors and switching sequences.

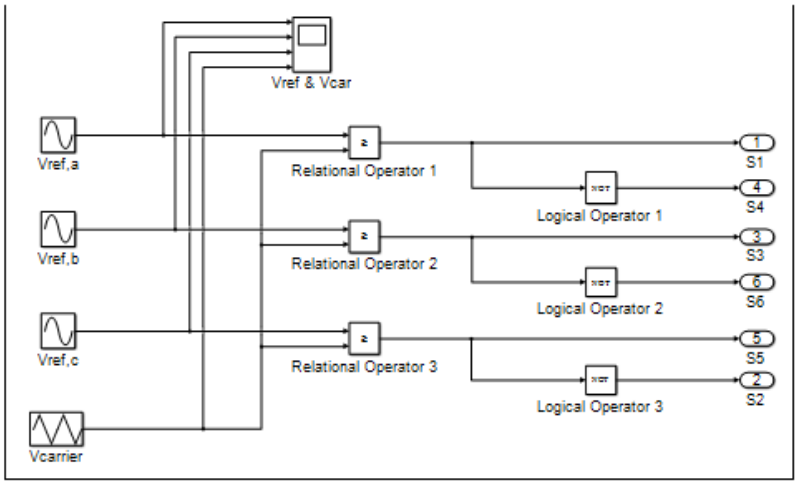

Figure 4: SPWM as modulator for pulses generation of the inverter system

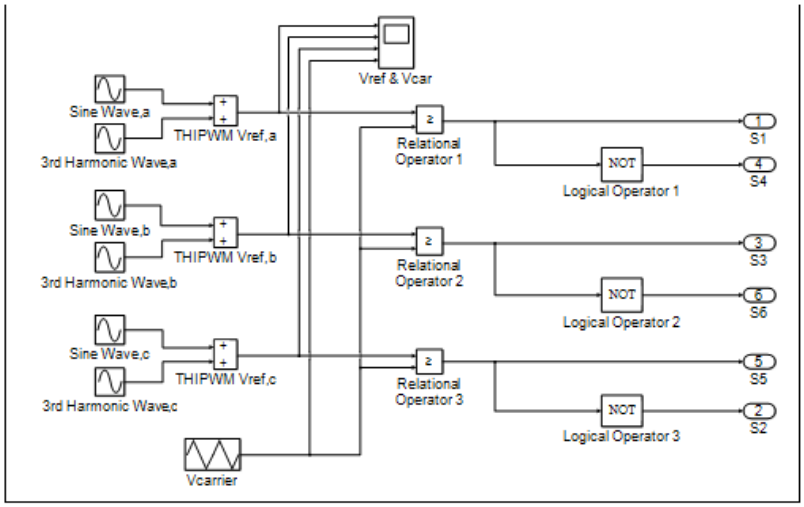

Figure 5: THIPWM modulator for pulses generation of the inverter system

3.2. Synchronous frame proportional-integral (PI) control for voltage control loop in standalone system

The conventional PI control transfer function is given in equation (7). This equation is expanded in synchronous-dq frame to improve the stability at the expense of response time and harmonic rejection (multi loop) [3].

The transfer function is:

$$G(s) = K_p + \frac{K_I}{s} \qquad (7)$$

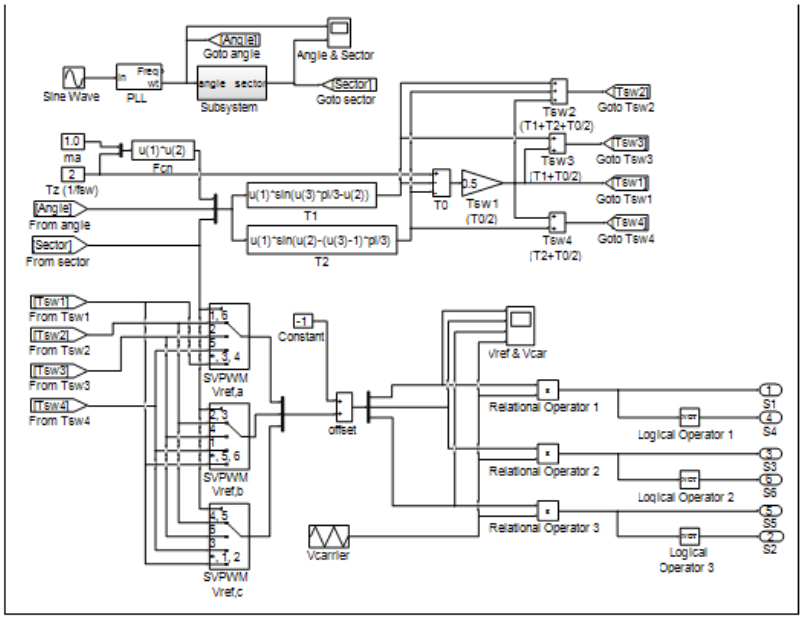

Figure 6: SVM as modulator to generate the gating pulses for inverter system

This work uses voltage-controlled synchronous-dq reference frame to control the desired fundamental output and frequency, the three-phase ac quantities are transformed into dc components to ensure any steady-state error is eliminated. Based on Figure 7, the inverter ac side dynamics in stand-alone mode can be expressed in the d-q axis reference frame as in (8) to (9). i_{cdq} is the capacitor current, v_{idq} is pre-filter inverter voltage, i_{odq} is load current and v_{odq} is load voltage in dq-quantities. L_f and C_f are the ac power filters at the load.

$$\frac{di_{cdq}}{dt} = \frac{1}{L_f}\left[v_{idq} + \omega L_f i_{oqd} - v_{odq}\right] \tag{8}$$

$$\frac{dv_{odq}}{dt} = \frac{1}{C_f}\left[i_{idq} - \frac{v_{odq}}{R_o} + \omega C_f v_{oqd}\right] \tag{9}$$

Let $U_d = i_{id} + \omega C_f v_{oq}$ and $U_q = i_{iq} + \omega C_f v_{od}$, therefore (8) and (9) can be written as:

$$\frac{dv_{odq}}{dt} = -\frac{v_{odq}}{R_o C_f} + \frac{U_{dq}}{C_f} \tag{10}$$

The variables U_d and U_q can be obtained from the proportional-integral (PI) controller in (7) as follows:

$$U_{dq} = k_p(v^*_{odq} - v_{odq}) + k_i \int (v^*_{odq} - v_{odq})dt \tag{11}$$

eplacing the integral parts of (11), with Z_d and Z_q, the following sets of equations are obtained:

$$U_{dq} = k_p(v^*_{odq} - v_{odq}) + Z_{dq} \tag{12}$$

$$\frac{dv_{odq}}{dt} = -\frac{(1 + R_o k_p)}{R_o C_f} v_{odq} + \frac{k_p v^*_{odq}}{C_f} + \frac{Z_{dq}}{C_f} \tag{13}$$

$$\frac{dZ_{dq}}{dt} = k_i(v^*_{odq} - v_{odq}) \tag{14}$$

Differential equations (11) to (14) can be written in state space form as:

$$\frac{d}{dt}\begin{bmatrix} V_{od} \\ V_{oq} \\ Z_d \\ Z_q \end{bmatrix} = \begin{bmatrix} -\dfrac{(1+R_o k_p)}{R_o C_f} & 0 & \dfrac{1}{C_f} & 0 \\ 0 & -\dfrac{(1+R_o k_p)}{R_o C_f} & 0 & \dfrac{1}{C_f} \\ -k_i & 0 & 0 & 0 \\ 0 & -k_i & 0 & 0 \end{bmatrix} \begin{bmatrix} V_{od} \\ V_{oq} \\ Z_d \\ Z_q \end{bmatrix} = \begin{bmatrix} \dfrac{k_p}{C_f} & 0 \\ 0 & \dfrac{k_p}{C_f} \\ k_i & 0 \\ 0 & k_i \end{bmatrix} \begin{bmatrix} V_{od} \\ V_{oq} \end{bmatrix} \quad (15)$$

The proposed voltage controller equations are written in (16) and illustrated in Figure 7. The voltage controller added feedforward terms($\omega C_f v_{oqd}$) with is applicable for both inverters

$$i_{idq} = U_{dq} - \omega C_f v_{oqd} = k_p(v^*_{odq} - v_{odq}) + k_i \int (v^*_{odq} - v_{odq})dt - \omega C_f v_{oqd} \quad (16)$$

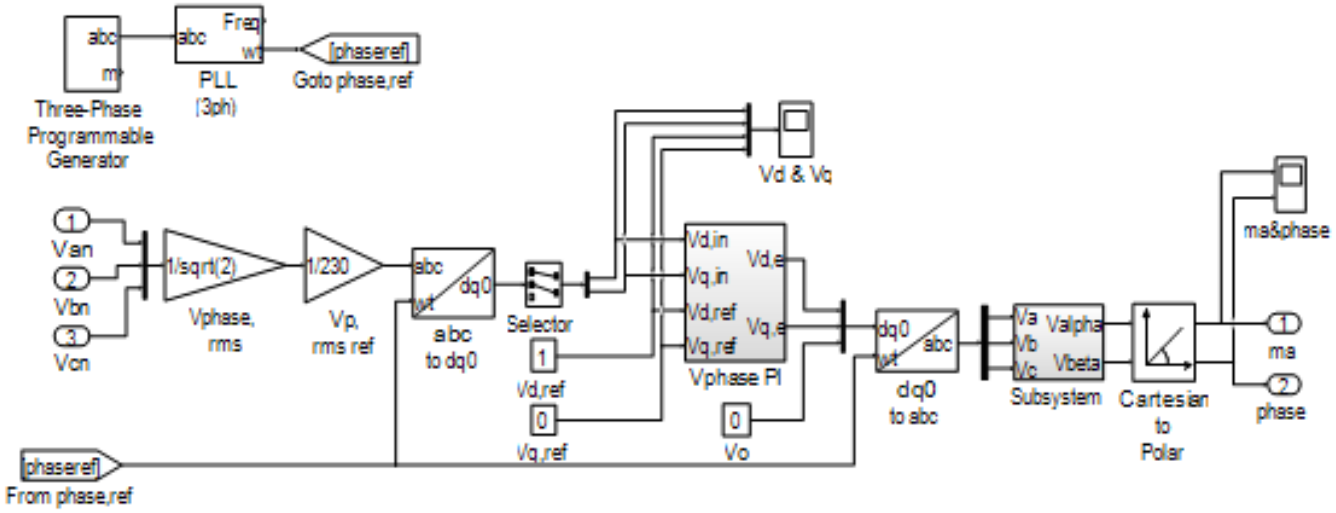

Figure 7: Proposed Voltage Control Loop using Synchronous Frame Proportional-Integral Control for VSI and CSI

Next, the proposed voltage control loop as in Figure 7 need to be controlled using proportional and integral control gain (K_p andK_i). Figure 8 shown the tuning process to obtain the optimized control gain in MATLAB/Simulink environment. The tuning process start with set the K_p to the lowest possible value and K_i is set to zero. Next, the value of K_p is gradually rise until it reached K_{max} where the maximum value that causes a sustained oscillation. This waveform can be viewed using scope display. Then, K_{max} is set as K_p, start to increase the value of K_i until an optimized time response of the control system is obtained. Even the control system achieves an optimized time response, the output might still have noise and oscillation. Thus, start to lower the value of K_p while maintaining the Ki to reduce the output noise and oscillation. Once an output waveform with optimized time response and lower noise are obtained, the values of K_p and K_i are considered as an optimized PI control gain for the control system. This process is completed and the proposed voltage control can be tested and analyzed with varying load parameters or different filter design values to see the limit of the obtained control gain.

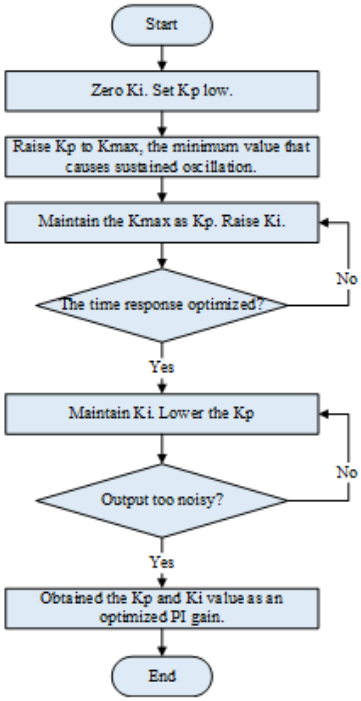

Figure 8: Tuning process to obtain an optimized PI control gain.

4. Result and discussion

4.1. Open loop verification of Case I, II and III

Table 2 lists the parameter used for evaluating the performance of the inverters in open-loop condition. As stated in Table 2, there are two conducted tests namely Cases I and II to investigate the relationship between modulation index, switching frequency, fundamental output components and harmonic elimination corresponding to these three modulation techniques. An interesting finding is presented in Case I which is three-phase CSI always provide a higher fundamental output as compared to three-phase VSI. This finding confirms that three-phase CSI have boosting capability on fundamental output as claimed by most of the past research works. Figure 9 presents the boosting capability of three-phase CSI by using different modulation techniques. From Table 3 and Figure 9, the main analysis found that three-phase CSI can provide a 52% to 58% higher fundamental output than VSI as the modulation index is varied. This boosting percentage satisfy the concern rise from this work on how much the boosting of CSI can be.

In Case III, the switching frequency, f_{sw} is varied as in Table 4 to investigate the relationship between the switching frequency with boosting capability and harmonic elimination. In this case, two groups of switching frequencies are implemented into three-phase VSI and CSI with different modulation techniques. Table 4 presents the group of switching frequencies, f_{sw} used in Case III. First group is the common switching frequencies ranging from 500Hz to 10kHz. Second group is the multiple of three switching frequency from 720Hz to 9kHz.

Figure 10 present the simulation result of Case III in term of fundamental magnitude of line-to-line voltage and percentage total harmonic distortion (%THD) for both inverters. In Figure 10, it shows the variation of switching frequencies do not have much effect on the boosting capability (are viewed in term of fundamental outputs) and harmonic elimination. Furthermore, by comparing fundamental output and THD based on type of modulation techniques, THIPWM and SVM always provide higher fundamental output and lower THD as compared to SPWM. It is found out in Figure

Table 2: System parameter of three-phase VSI and CSI based on Case I and II

Parameter	**Three-phase VSI**		**Three-phase CSI**	
	Case I	Case II	Case I	Case II
Input voltage, V_{dc}(V)	700V	700	-	-
Input current, I_{dc}(A)			8A	8A
Modulation index, m_a	0.05 – 1.0	Choosen m_a	0.05 – 1.0	Choosen m_a
Switching frequency (f_{sw})	2kHz	500Hz-10kHz	2kHz	500Hz-10kHz

Table 3: Boosting capability of three-phase CSI compared to three-phase VSI.

m_a	SPWM			THIPWM			SVM		
	$V_{phasevoltage}$			$V_{phasevoltage}$			$V_{phasevoltage}$		
	VSI	CSI	Boosting (%)	VSI	CSI	Boosting (%)	VSI	CSI	Boosting (%)
0.05	20.95	26.25	**25.298**	19.60	30.66	**56.429**	20.33	31.45	**54.697**
0.10	34.96	53.27	**52.374**	40.37	63.25	**56.676**	40.49	62.80	**55.100**
0.20	68.59	108.30	**57.895**	80.35	126.40	**57.312**	81.54	125.60	**54.035**
0.30	107.90	163.70	**51.715**	121.90	188.80	**54.881**	120.50	188.30	**56.266**
0.40	139.70	217.80	**55.906**	161.30	252.30	**56.417**	161.80	251.30	**55.315**
0.50	174.90	272.80	**55.975**	202.60	313.70	**54.837**	202.30	315.20	**55.808**
0.60	209.20	326.70	**56.166**	241.80	376.30	**55.624**	243.00	377.60	**55.391**
0.70	246.90	380.40	**54.070**	283.00	439.50	**55.300**	283.80	440.50	**55.215**
0.80	279.60	436.90	**56.259**	323.50	502.60	**55.363**	323.00	503.90	**56.006**
0.90	315.10	490.10	**55.538**	363.50	566.70	**55.901**	363.30	567.30	**56.152**
1.00	351.00	546.40	**55.670**	404.50	630.30	**55.822**	404.30	629.40	**55.676**

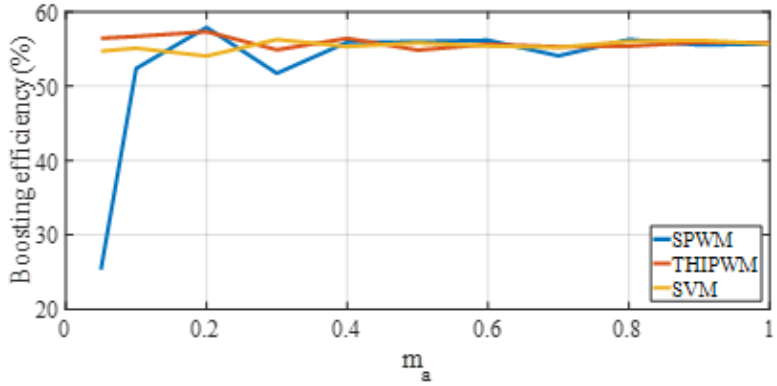

Figure 9: Boosting capability of three-phase CSI by using different modulation techniques.

10(a), no matter the modulation techniques used, the fundamental output and THD of three-phase CSI always higher than three-phase VSI. Thus, 3kHz switching frequency is selected (as highlighted in box in Figure 10) to implemented into three-phase VSI and CSI in closed-loop system.

The system parameter of three-phase SVM VSI and CSI with PI control system are show in Table 5. The analysis continued with investigation of the boosting capability of CSI in the proposed

Table 4: Group of switching frequency, f_{sw} for Case III

Common switching frequency (Hz)	Multiple of three switching frequency (HZ)
500	720
1000	1080
2000	1500
4000	3000
5000	4500
7000	5400
8000	6000
10000	7200
-	8100
-	9000

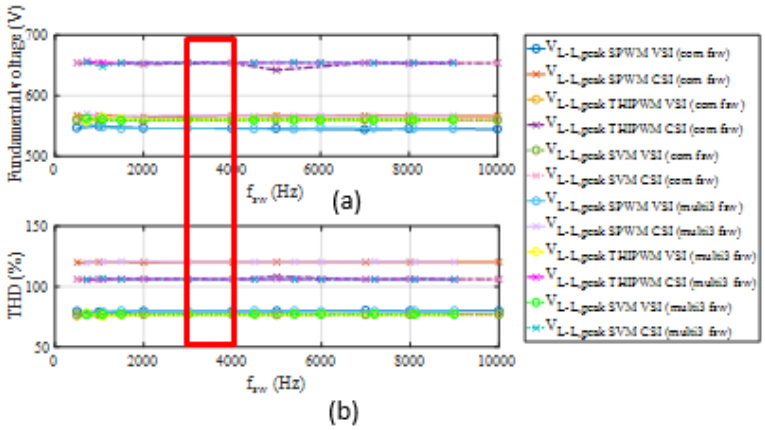

Figure 10: (a) Line-to-line voltage fundamental output and (b) THD of three-phase VSI and CSI for Case III. 4.2 Closed-loop verification of synchronous frame PI Control of VSI and CSI system

voltage control closed-loop verification.

Table 5: System parameter of three-phase SVM VSI and CSI with voltage controlled system

Parameter	Three-phase SVM VSI	Three-phase SVM CSI
$\mathbf{P_{rated}}$ (W)	2kW	2kW
Fundamental frequency, $\mathbf{f_o}$(Hz)	50Hz	50Hz
Input voltage, $\mathbf{V_{dc}}$(V)	700V	-
Input current, $\mathbf{I_{dc}}$ (A)	-	8A
Load (Ω)	79	79
$\mathbf{m_a}$	0.8	0.6
$\mathbf{f_{sw}}$**(Hz)**	3kHz	3kHz
LC or CL filter	$L_f = 8mH, C_f = 20\mu F$ LC filter	$C_f = 6\mu F, L_f = 30mH$ CL filter
PI control gain	$K_p = 1.8, K_i = 600$	$K_p = 0.7, K_i = 250$

Figure 11 presents the $V_{d,in}$ and $V_{q,in}$ signal that generated by PI control system of three-phase VSI (Figure 11(a)) and CSI (Figure 11(b)). Next, the output waveform of three-phase VSI and CSI with PI control system are present in Figure 12. From Figure 11 and 12, both PI control system in

three-phase VSI and CSI take around 0.02s to reach a stable state. For three-phase VSI, the designed PI control system have oscillation at starting period in $V_{d,in}$ and $V_{q,in}$ signal and this cause a starting voltage spikes and current spikes in the phase voltage, phase current and line-to-line voltage, see Figure 12(a) and (b). Besides, the output active power of three-phase VSI even reach a reach an energy spikes highest to 3500W as shown in Figure 12(c). These voltage, current and energy spikes may damage the sensitive components in three-phase inverter or the loads. Thus, system protections are required for the voltage, current and output power spikes issues. Some system protections for instance adding suitable ac power filters are recommended to solve this issue.

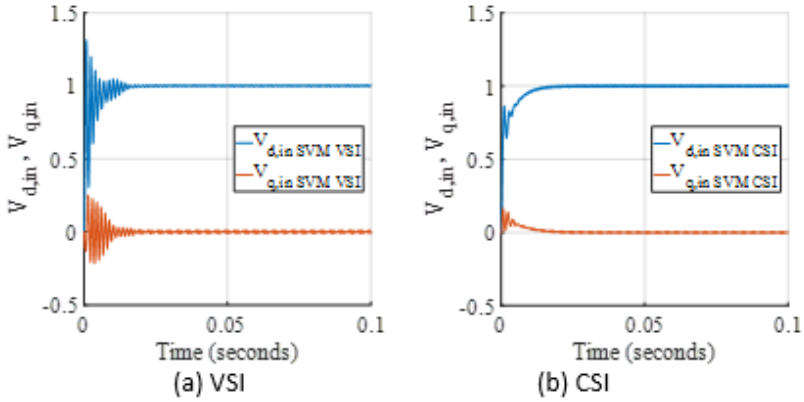

Figure 11: $V_{d,in}$ and $V_{q,in}$ of PI control system for three-phase VSI and CSI.

Table 6 shown the output range based on the proposed voltage control system limitation for the inverters. In Table 6, it clearly shows that three-phase CSI can achieve an output in a wider range by using smaller control gains as compared to gains used for VSI.

Table 6: Output range based on proposed voltage control system limitation.

	Three-phase SVM VSI	**Three-phase SVM CSI**
PI control gain	$K_p = 1.8, K_i = 600$	$K_p = 0.7, K_i = 250$
Load (Ω)	79Ω	79Ω
$\mathbf{V_{d,ref}}$	0.1 - 1.2	0.1 - 1.9
$\mathbf{m_a}$	0.08 - 0.95	0.05 - 0.98
$\mathbf{V_{\phi,rms}(V)}$	$23V_{rms} - 276V_{rms}$	$23V_{rms} - 437V_{rms}$
$\mathbf{I_{\phi,rms}}$ (A)	0.2912A - 3.4920A	0.2912A - 5.5310A
$\mathbf{V_{L-L,rms}(V)}$	$39.84V_{rms} - 478V_{rms}$	$39.85V_{rms} - 756.9V_{rms}$

In this analysis, the output reference, $V_{d,ref}$ in the voltage-controlled system start to increase from 0.1pu. The control signal generated by the control system are shown in Figure 13. Based on Figure 13(a), the voltage controlled of the three-phase inverter able to track the $V_{d,ref}$ until it over the system limitation, where the overmodulation occurs. For three-phase VSI, the voltage-controlled system generates an output of $m_a > 1$ which caused overmodulation when $V_{d,ref}$=1.3, thus results in oscillation of $V_{d,in}$ and m_a signal as shown in Figure 13(b). For three-phase CSI, the voltage-controlled system generates an $m_a > 1$ at $V_{d,ref}$=2.0. This overmodulation also cause an oscillation $V_{d,in}$ and m_a signal occurs. This finding determine that the proposed control of VSI reach its limitation at $V_{d,ref}$=1.2 while for CSI, it expand the limitation where it hit the limit when $V_{d,ref}$=1.9 as shown in Figure 13(b).

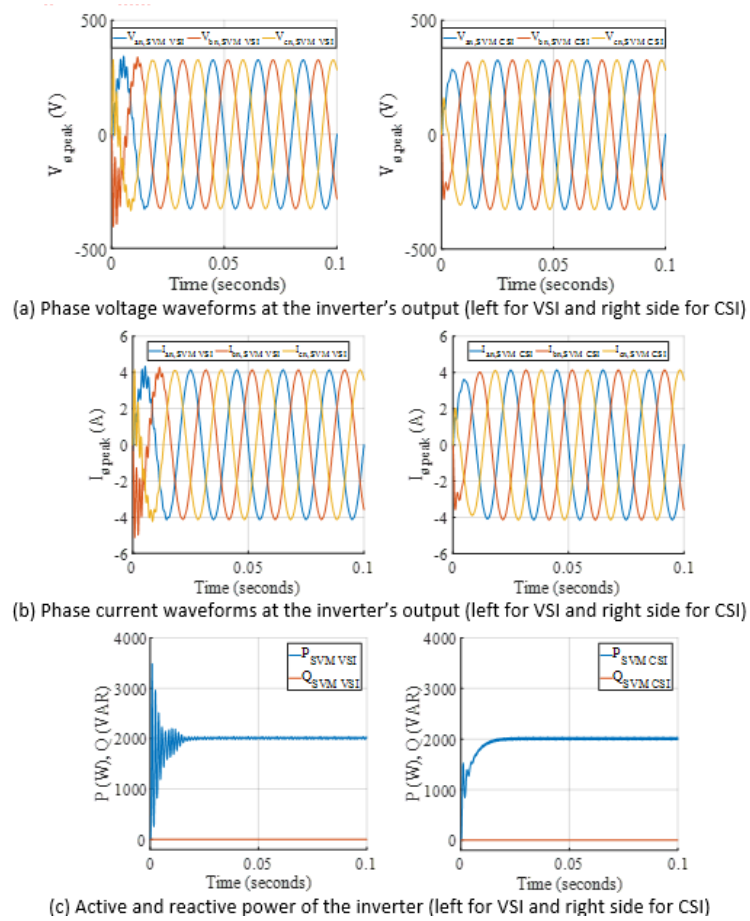

Figure 12: Output waveform of three-phase VSI and CSI with proposed voltage control system.

The closed-loop voltage-controlled system is hybrid for both inverters with only slight different of their control gains. As stated in Table 6, the control gains for VSI are $K_p = 1.8$ and $K_i = 600$ while for three-phase CSI, the control gains are $K_p = 0.7$ and $K_i = 250$. This is the second important finding related to CSI whereby despite of smaller control gains used for CSI, it able to provides a wider output phase voltage range as compared to three-phase VSI as stated in Table 6. In term of output waveform, VSI output waveform suffer oscillation at the starting period, which may cause the spiking or overshoot issues as shown in Figure 13. These spiking and overshoot issues may damage the sensitive components and system. Thus, three-phase VSI required larger filter requirement to solve these issues. For three-phase CSI, the output waveforms and control signal have a smooth inclined or decay at the starting period or even when a transient occurred as shown in Figure 13. Hence, three-phase CSI can provide a better output waveform and smaller filter sizing as compared to three-phase VSI.

5. Conclusion

Voltage and current source inverter are viable option for interfacing unit between dc renewable system and local loads in standalone application. The comparative analysis of both inverters was done in open-loop steady state and closed-loop voltage-controlled conditions. In this comparative analysis, three-phase CSI present promising voltage boosting capability with an incremental between 52% to 58% than VSI and could achieve a wider output phase voltage range by using a smaller proportional-integral control gain. It is proved that CSI able to perform relatively the same as VSI.

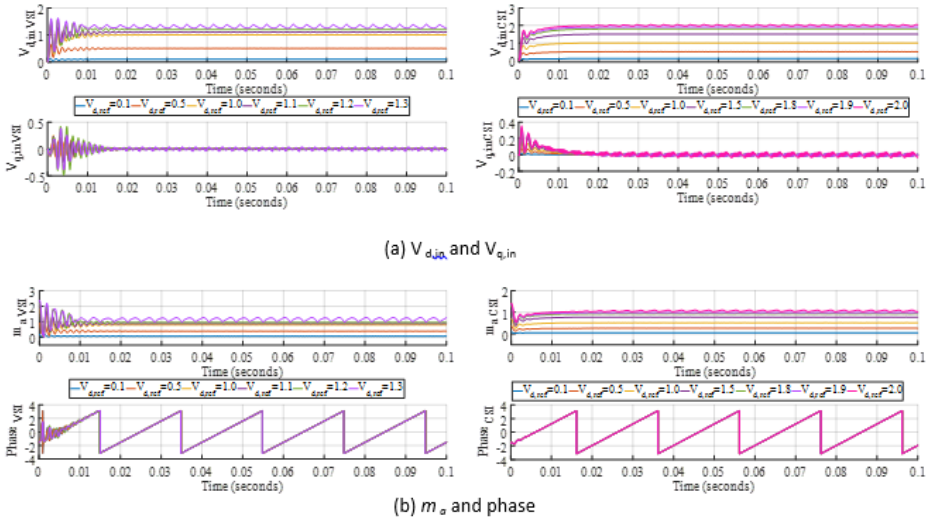

Figure 13: Control signal of PI control system for three-phase VSI and CSI (a) $V_{d,in}$ and $V_{q,in}$ (b) m_a and phase

These promising features become the advantages of three-phase CSI to be implemented for some industrial application particularly in medium to high power application. It is hope that this research can be a reference for the researcher and designer to do selection on suitable inverter topology with correct modulation techniques and dedicated control system.

Acknowledgement

The authors would like to acknowledge the Research Management (RMC) Universiti Malaysia Perlis, Perlis, Malaysia and the Ministry of Education, Malaysia (MOE) for the financial support of this research. This research is supported by MOE under Fundamental Research Grant Scheme (FRGS) with project code: FRGS/1/2020/TK0/UNIMAP/02/100 (9003-00851).

References

[1] S.A. Azmi, M.A. Roslan, G.P. Adam and B.W. Williams. *DC Current Offset Compensation Technique for Grid Connected Inverters*, 9th International Conference on Power Electronics - ECCE Asia: Green World with Power Electronics (ICPE 2015-ECCE Asia) (2015) 617-623.

[2] S. A. Azmi, K. H. Ahmed, S. J. Finney and B. W. Williams, *Comparative analysis between voltage and current source inverters in grid-connected application*, In IET Conference on Renewable Power Generation, (2011) 101–101, https://doi.org/10.1049/cp.2011.0138.

[3] S.A. Azmi, M.F.N. Tajuddin, M.F. Mohamed and L.J. Hwai, *Multi-loop Control Strategies of Three- phase Two-level Current Source Inverter for Grid Interfacing Photovoltaic System*, 3rd IEEE Conference on Energy Conversion (CENCON2017), (2017) 227-282.

[4] A. Benslimane, J. Bouchnaif, M. Essoufi, B. Hajji, and L. el Idrissi, *Comparative study of semiconductor power losses between CSI-based STATCOM and VSI-based STATCOM, both used for unbalance compensation*, Protection and Control of Modern Power Systems, 5(1) (2020) 4. https://doi.org/10.1186/s41601-019-0150-4.

[5] H. Dai, R. A. Torres, W. Lee, T. M. Jahns, and B. Sarlioglu, *Integrated Motor Drive using Soft-Switching Current-Source Inverters with SiC- And GaN-based Bidirectional Switches*, In ECCE 2020 - IEEE Energy Conversion Congress and Exposition (2020). 2372–2378, https://doi.org/10.1109/ECCE44975.2020.9236394.

[6] V. Delli Colli, P. Cancelliere, F. Marignetti and R. Di Stefano, *Influence of voltage and current source inverters on low-power induction motors*, IEE Proceedings - Electric Power Applications, 152(5) (2005) 1311, https://doi.org/10.1049/ip-epa:20045243.

[7] E. Fernandez, A. Paredes, L. Romeral, and V. Sala, *Analysis of power converters with devices of sic for applications in electric traction systems*, In 2016 IEEE International Power Electronics and Motion Control Conference, (2016) 267–272, IEEE. https://doi.org/10.1109/EPEPEMC.2016.7752009.

[8] K. G. Jayanth, V. Boddapati, and R. S. Geetha, *Comparative study between three-leg and four-leg current-source inverter for solar PV application*, In 2018 International Conference on Power, Instrumentation, Control and Computing (PICC) , (2018) 1–6, IEEE. https://doi.org/10.1109/PICC.2018.8384793.

[9] S. Kouro, J. I. Leon, D. Vinnikov, and L. G. Franquelo, *Grid-connected photovoltaic systems: An overview of recent research and emerging PV converter technology*, IEEE Industrial Electronics Magazine, 9(1) (2015) 47–61. https://doi.org/10.1109/MIE.2014.2376976

[10] P. Killeen, and D. C. Ludois, E*valuation of Drive Topologies for Macro Scale Synchronous Electrostatic Machines*, In 2020 22nd European Conference on Power Electronics and Applications, (2020) 1–10, https://doi.org/10.23919/EPE20ECCEEurope43536.2020.9215906

[11] F. Lin Luo, and H. Ye, *Advanced DC/AC Inverters: Applications in Renewable Energy*, CRC Press Taylor & Francis Group.

[12] J. W. Makhubele and K. A. Ogudo, *Analysis on Basics of Modulation Techniques for AC Drive on Efficiency Improvements*, In 2020 IEEE PES/IAS PowerAfrica, (2020) 1–5.

[13] G. Migliazza, E. Lorenzani, F. Immovilli, and G. Buticchi, *Single-Phase Current Source Inverter with Reduced Ground Leakage Current for Photovoltaic Applications*, Electronics, 9(10) (2020) 1618. https://doi.org/10.3390/electronics9101618.

[14] H. Muhammad, P. D. Rashid, *Power Electronics Handbook (4th ed.)*, (2018). https://doi.org/10.1109/PowerAfrica49420.2020.9219886.

[15] K. B. Nagasai, and T. R. Jyothsna, *Harmonic Analysis and Application of PWM Techniques for Three Phase Inverter*, International Research Journal of Engineering and Technology, (2016) 2395–56.

[16] S. Pradeepa, P. Kumar, and G. Prakash, *Adoption of SVPWM Technique to CSI and VSI*, In 2018 3rd International Conference for Convergence in Technology (I2CT) (2018). 1–6. https://doi.org/10.1109/I2CT.2018.8529694.

[17] S. A. Ravindra and S. M. Ravindra, *Grid-Connected Photo-Voltaic System By Using Different PWM Techniques For Inverter Control*, In 2020 IEEE PES/IAS PowerAfrica , 1–4, https://doi.org/10.1109/PowerAfrica49420.2020.9219922.

[18] A Vandermeulen and J. Maurin, *Current source inverter vs*, Voltage source inverter topology, (2014) 1–8.

[19] E. P. Wiechmann, P. Aqueveque, R. Burgos, and J. Rodriguez, *On the Efficiency of Voltage Source and Current Source Inverters for High-Power Drives. IEEE Transactions on Industrial Electronics*, 55(4) (2008) 1771–1782. https://doi.org/10.1109/TIE.2008.918625.

[20] K. Zeb, W. Uddin, M. A. Khan, Z. Ali, M. U. Ali, N. Christofides, and H. J. Kim, *A comprehensive review on inverter topologies and control strategies for grid connected photovoltaic system*, Renewable and Sustainable Energy Reviews, 94 (2018) 1120–1141. https://doi.org/10.1016/j.rser.2018.06.053.